Title
Cyclic Fatigue-Crack Propagation in Ceramics: Long and Small Crack Behavior

Authors
Steffen, A.A.
Dauskardt, R.H.
Ritchie, R.O.

Publication Date
1989-12-01

Center for Advanced Materials

CAM

Presented at the FATIGUE 90, Fourth International Conference on Fatigue and Fatigue Thresholds, Honolulu, Hawaii, July 15–20, 1990, and to be published in the Proceedings

Cyclic Fatigue-Crack Propagation in Ceramics: Long and Small Crack Behavior

A.A. Steffen, R.H. Dauskardt, and R.O. Ritchie

December 1989

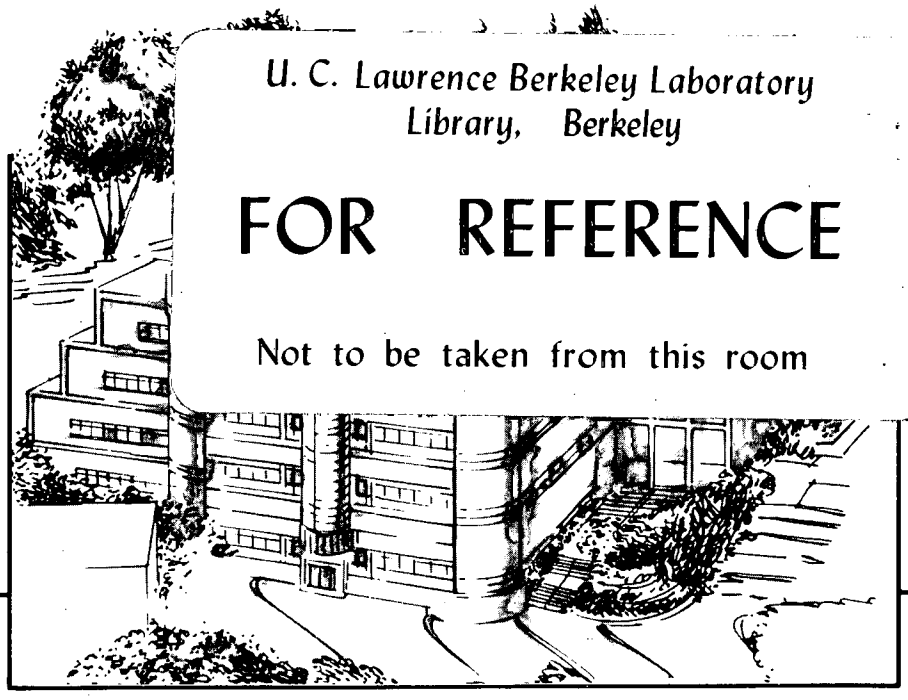

Materials and Chemical Sciences Division

Lawrence Berkeley Laboratory • University of California

ONE CYCLOTRON ROAD, BERKELEY, CA 94720 • (415) 486-4755

Prepared for the U.S. Department of Energy under Contract DE-AC03-76SF00098

DISCLAIMER

LBL-28243

CYCLIC FATIGUE-CRACK PROPAGATION IN CERAMICS: LONG AND SMALL CRACK BEHAVIOR

A. A. Steffen, R. H. Dauskardt and R. O. Ritchie

Center for Advanced Materials, Lawrence Berkeley Laboratory
and
Department of Materials Science and Mineral Engineering
University of California, Berkeley, CA 94720

December 1989

to be presented at *FATIGUE 90, Fourth International Conference on Fatigue and Fatigue Thresholds*, July 15-20, 1990, Honolulu, Hawaii

Work supported by the Director, Office of Energy Research, Office of Basic Energy Sciences, Materials Sciences Division of the U.S. Department Energy under Contract No. DE-AC03-76SF00098.

CYCLIC FATIGUE-CRACK PROPAGATION IN CERAMICS: LONG AND SMALL CRACK BEHAVIOR

A. A. Steffen, R. H. Dauskardt and R. O. Ritchie*

Center for Advanced Materials, Lawrence Berkeley Laboratory, and Department of Materials Science and Mineral Engineering, University of California, Berkeley, CA 94720

Stress/life (S/N) and cyclic fatigue-crack growth properties are studied in a Mg-PSZ, with particular reference to the role of crack size. S/N data from unnotched specimens show markedly lower lives under tension-compression compared to tension-tension loading; "fatigue limits" (at 10^8 cycles) for the former case approach 50% of the tensile strength. Under tension-tension loading, cyclic crack-growth rates of "long" (>3 mm) cracks are found to be power-law dependent on the stress-intensity range ΔK with a fatigue threshold, ΔK_{TH}, of order 50% K_c. Conversely, naturally-occurring "small" (1 to 100 μm) surface cracks were observed to grow at ΔK levels some 2 to 3 times smaller than ΔK_{TH}. The implications of such data for structural design with ceramics is briefly discussed.

INTRODUCTION

Recently, there has been increasing concern over the apparently anomalous behavior of "small" fatigue cracks in the engineering design and life prediction of structures (e.g. 1). Where cracks are physically small ($\leq$ 500 μm) or approach the dimensions of microstructure or local crack-tip inelasticity, crack propagation rates are known to exceed those of "long" ($\geq$ 3 mm) cracks at equivalent applied stress-intensity ranges ΔK, and more importantly to occur at ΔK levels *less than* the fatigue threshold ΔK_{TH}, below which fatigue cracks are presumed dormant. Since damage-tolerant design and life-prediction procedures generally preclude such early crack growth and invariably utilize conventional long-crack data, the accelerated and sub-threshold growth of small cracks provides a strong potential for non-conservative prediction.

The small-crack effect primarily arises from the restricted influence of crack-tip shielding mechanisms (which act to reduce the near-tip "driving force" (1,2)) in cracks of limited wake. In this context, "small" is best defined as comparable in size to the equilibrium extent of shielding behind the crack tip. The principal mechanism of such shielding in metal fatigue is generally crack closure, i.e., premature contact between

crack surfaces during the cycle due, for example, to wedging from fracture-surface asperities or corrosion debris (1,3). Accordingly, at a given applied stress intensity, a small crack may experience a larger *local* (near-tip) "driving force" than a long crack due to less wake shielding, analogous to the resistance-curve (R-curve) phenomenon in toughness tests.

Since many advanced ceramic materials are similarly toughened by shielding mechanisms (2), e.g., transformation toughening or fiber/whisker bridging, small-crack effects are expected to be equally important. In fact, fracture toughness tests on transformation-toughened Mg-PSZ show R-curves for small ($< 400\ \mu m$) surface cracks to occur at much lower K levels than those for long cracks (4). Moreover, for subcritical cracking under monotonic loads, results for $\sim 100\ \mu m$ long cracks growing out of residual stress fields around hardness indents in soda-lime glass (5), and ~20-200 μm long surface cracks in bend specimens of Mg-PSZ (6), both show sub-threshold crack-growth behavior with a negative dependency on K, akin to behavior in metals (1). Similarly for fatigue, small-crack data have been reported for surface cracks ($< 300\ \mu m$) in Ce-PSZ (7), for indentation cracks ($< 50\ \mu m$) in Al_2O_3 and Si_3N_4 (8), and for corner cracks ($< 250\ \mu m$) in LAS/SiC-fiber glass-ceramics (9). Although growth rates in the latter three ceramics all show a negative dependency on K, no comparisons have been made with long-crack fatigue data in the same material.

The objective of the present study is to investigate the cyclic fatigue behavior of a well characterized ceramic, Mg-PSZ, with reference to the role of microstructurally-small cracks. Fatigue properties are examined in terms of classical stress/life (S/N) and crack-propagation rate data; in the latter case results are compared for long pre-existing, through-thickness cracks with naturally-occurring small surface cracks.

EXPERIMENTAL PROCEDURES

The material examined was a partially-stabilized zirconia, containing 9 mol% magnesia (Mg-PSZ, Nicra) (10). Sintering/heat treatment in the cubic phase field, followed by controlled cooling and subeutectoid aging at 1100°C for 3 to 24 h, resulted in a series of microstructures consisting of cubic ZrO_2 grains (diameter $\sim 50\ \mu m$), with ~35-40 vol% lens-shaped tetragonal precipitates (maximum size ~300 nm). The tetragonal precipitates undergo a stress-induced martensitic transformation to a monoclinic phase in the high stress field near the crack tip. The resultant dilatant transformation zone in the wake of the crack exerts compressive tractions on the crack surfaces and shields the

crack tip from the applied (far-field) stresses (11,12). The crack-tip stress intensity, K_{tip}, is therefore reduced from the applied (far-field) K by an amount, K_s, such that:

$$K_{tip} = K - K_s , \quad (1)$$

where the shielding stress intensity K_s is dependent upon the volume fraction, f, of the transforming phase within the zone, the width w of the zone, and the dilational component of the transformation strain ε^T (11):

$$K_s = A\, E'\, \varepsilon^T\, f\, w^{1/2} , \quad (2)$$

with $E' = E/(1 - \nu^2)$, E is Young's modulus, ν is Poisson's modulus, and the constant A is dependent upon ε^T and the zone shape.

The microstructures examined and their room-temperature properties are listed in Table 1; these structures vary from the peak toughened (TS-grade) condition ($K_c \sim 16$ MPa$\sqrt{m}$) to an overaged (non-transformation-toughened) condition ($K_c \sim 3$ MPa$\sqrt{m}$).

TABLE 1 - Heat Treatments and Tensile Properties of Mg-PSZ

Condition (grade)	Heat Treatment	Young's Modulus, E (GPa)	Approx. Tensile Strength (MPa)	Fracture Toughness† K_i (MPa$\sqrt{m}$)	Fracture Toughness† K_c (MPa$\sqrt{m}$)
overaged	24 h at 1100°C	<200	300	2.5	2.9
low toughness (AF)	as received	208	300	3.0	5.5
mid toughness (MS)	3 h at 1100°C	208	600	3.0	11.5
peak toughness (TS)	7 h at 1100°C	208	400	4.0	16.9

†K_i and K_c are the initiation and plateau toughness values from R-curves.

S/N tests were performed on 5-mm-thick unnotched cantilever-bend specimens (9 mm wide, 70 mm long), polished to 1 μm and cycled under tension-compression (stress ratio $R = \sigma_{min}/\sigma_{max} = -1$) and tension-tension ($R = 0$) loading in controlled ambient-temperature air (22°C, 45% relative humidity) at a sinsuoidal frequency of 100 Hz. Data are presented as cycles to failure, N_f, as a function of the maximum applied stress, σ_{max}, on the outer specimen surface.

Fatigue-crack propagation data for naturally-occurring small ($< 100\ \mu m$) surface cracks were determined by monitoring the top surface of bend specimens used in the S/N tests. Specimens were periodically removed and optically examined using Normarski interference microscopy. Tests were interrupted after ~100 cycles to determine damage accumulation during initial loading and after subsequent 10^2 to 10^3 cycle intervals until failure. Small-crack lengths could be readily detected by digitizing the optical micrographs using an image analyzer, with a resolution better than $\pm$ 0.5 μm. Owing to crack meandering, surface crack lengths were taken as the projected crack length normal to the direction of the bending stress. Crack-growth rates were determined over the range 10^{-13} to 10^{-6} m/cycle from crack length/number of cycles (a vs. N) curves. Stress-intensity factors were computed from linear-elastic solutions (13) for three-dimensional semi-elliptical surface cracks in bending in terms of crack depth, a, crack length, c, elliptical parametric angle, ϕ, shape factor, Q, specimen width, t, specimen thickness, B, and remote (outer fiber) bending stress, σ_b:

$$K = H_c \sigma_b (\pi a/Q)^{1/2} F(a/c, a/t, c/b, \phi) \qquad (3)$$

where H_c is the bending multiplier and F is the boundary correction factor. Eq. 3 is valid for $0.2 \leq a/c \leq 1$, $0 \leq u \leq 90°$ at $c/b \leq 0.5$. Based on examination of typical cracks, a/c ratios were found to be of the order of 0.8. Crack-growth rates (da/dN) are presented in terms of the maximum stress intensity, K_{max}, from the tensile portion of the cycle, calculated $a/c = 0.8$ at $\phi = 90°$.

Fatigue-crack propagation studies for long (>3 mm) cracks were performed on 3-mm thick compact C(T) specimens, which were cycled at R = 0.1 with a sinsuoidal frequency of 50 Hz (14-16). Crack-growth rates, over the range ~10^{-11} to 10^{-5} m/cycle were determined under automated ΔK-decreasing and ΔK-increasing conditions, with a normalized K gradient of $0.08 mm^{-1}$. An electrical-resistance technique was employed to monitor crack length (with a resolution better than 5 μm) using ~0.1-μm NiCr films, evaporated onto the specimen surface. Crack-growth rate data are presented in terms of the maximum and alternating ($\Delta K = K_{max} - K_{min}$) stress intensities.

RESULTS AND DISCUSSION

S/N Fatigue: S/N curves for the overaged and MS-grade material, are shown in Fig. 1 for both tension-compression (R= -1) and tension-tension (R = 0) loading. Similar to prior results in PSZ (17) and Si_3N_4 (18,19), cycling in tension and compression is clearly more damaging than in cyclic tension. The MS-grade material appears to show evidence of a "fatigue limit" of approximately 300 MPa (at 10^8 cycles with R = -1); similar to classical behavior of steels, this is roughly 50% of the tensile strength. Failures in the overaged material were observed at significantly lower stress levels.

The more damaging nature of tension-compression cycling was also apparent from a far higher density of microcracks and surface distortions observed on the tensile surfaces of MS-grade specimens after cycling at R = -1 compared to R = 0. Out-of-plane deformation in the transformation zones surrounding microcracks was highlighted using Nomarski interference techniques. The overaged condition showed a markedly lower density of microcracks.

The present S/N data is compared in Fig. 1 with previous results (17,20) for Mg-PSZ (Nicra MS-grade), tested in both low-cycle flexural bending (R = 0 and 0.86, frequency 0.03-0.16 Hz) and high-cycle rotating bending (R = -1, frequency 100 Hz). Despite the obvious scatter, the results at both R ratios are comparable with the present data.

Fatigue-Crack Propagation: Small Cracks: Crack length vs. (log) number of cycles curves, derived from monitoring the top surface of the bend specimens, were derived for the MS-grade Mg-PSZ at R = 0 and -1. Small cracks were seen to grow at progressively decreasing growth rates with increase in size. Moreover, growth rates under tension-tension conditions were somewhat slower than in tension-compression, consistent with the longer fatigue lives for specimens cycled at R = 0.

Crack-growth rates, plotted as a function of K_{max} using Eq. 3, are shown in Fig. 2. Similar to reports for Al_2O_3, Si_3N_4 and LAS/SiC_f ceramics (8,9), and for metals (1), small-crack growth rates display a negative, non-unique, dependency on K. Growth rates, however, appear to be sensitive to the level of applied stress, and, at the same stress level, slower under tension-tension compared to tension-compression loading.

Fatigue-Crack Propagation: Long Cracks: Long-crack fatigue-crack growth rates for Mg-PSZ in tension-tension are shown in Fig. 3a; data for the MS-grade microstructure are compared with corresponding small-crack results in Fig. 2. The long-crack data conform to a Paris power-law relationship:

$$da/dN = C(\Delta K)^m . \quad (4)$$

The exponent, m, varies between 21 to 42; the constant C appears to scale inversely with fracture toughness. For each structure, an apparent fatigue threshold, ΔK_{TH}, can be defined below $\sim 10^{-10}$ m/cycle. The value of ΔK_{TH} is approximately 50% K_c. It should also be noted that, despite the absence of transformation "plasticity", the overaged material exhibits fatigue-crack growth behavior with a similar power-law dependency.

Fatigue fracture surfaces were primarily transgranular with crack paths showing evidence of crack deflection, branching and uncracked-ligament bridging behind the crack tip. The degree of tortuosity appeared to diminish progressively with decreasing toughness, as evidenced by the comparatively linear crack paths in the overaged structure.

It is clear from Fig. 4a that with increasing degrees of crack-tip shielding from transformation toughening, resistance to cyclic fatigue-crack extension in Mg-PSZ is increased. In fact, it has been shown (16) that such crack-growth data for the four microstructures can be normalized by characterizing in terms of the near-tip stress-intensity range, ΔK_{tip}, which accounts for such transformation shielding (Fig. 3b):

$$\Delta K_{tip} = K_{max} - K_s , \quad (5)$$

where K_s is computed using the integrated form of Eq. 2 from Raman spectroscopy measurements of the transformation-zone size (21).

Small- and long-crack growth rates for the MS-grade microstructure are compared in Fig. 2. Here the diminished role of transformation shielding of small cracks leads to significantly faster crack-growth rates. Akin to behavior in metals (1), small cracks propagate at stress-intensity levels well below the long-crack fatigue threshold (specifically at K_{max} levels of ~ 1.6 MPa$\sqrt{m}$). Crack growth appears to begin at stress intensities close to those of the near-tip ΔK_{tip} relationship for long cracks (c.f.,

Fig. 3b), and subsequently to grow at progressively decreasing growth rates with increasing applied stress-intensity levels.

For structural design, such small-crack data represent a problem. In safety-critical applications involving metallic structures, damage-tolerant approaches are often used which rely on the integration of crack-velocity/stress-intensity (v/K) curves (e.g., Eq. 4) to estimate the time or cycles for a presumed initial crack to grow to failure. Although such cyclic v/K data are now avaliable for ceramics, the approach may prove difficult to utilize in practice because of the large power-law dependence of growth rates (da/dN) on ΔK, which implies that the estimated life will be proportional to the reciprocal of the applied stress raised to a large power. The alternative procedure is to redefine the critical crack size in terms of the fatigue threshold ΔK_{TH}, below which crack growth is presumed dormant; this in essence is a crack-initiation criterion where ΔK_{TH} is taken as the effective toughness. However, on the basis of the small-crack data generated in the present work (Fig. 2), this approach may also be highly non-conservative.

CONCLUSIONS

Based on a study of the cyclic properties of Mg-PSZ ceramics, involving characterization of fatigue-crack propagation behavior for both long (> 3 mm) and microstructurally-small (< 100 μm) cracks and of stress/life (S/N) curves, the following conclusions can be made:

1. S/N data derived from unnotched bend specimens indicate that fatigue lifetimes are significantly shorter in tension-compression (R = -1) compared to tension-tension (R = 0) loading. Similar to steels, at R = -1 the "fatigue limit" at 10^8 cycles approaches 50% of the tensile strength.

2. Fatigue-crack growth rates for long cracks are found to be power-law dependent upon the stress-intensity range with an exponent between 21 and 42. Slowest growth rates are shown in structures with the highest toughness K_c; values of the threshold, ΔK_{TH}, approach 50% of K_c.

3. Fatigue-crack growth rates for naturally-occurring small cracks are found to occur at ΔK levels significantly smaller than ΔK_{TH}; moreover, similar to metals, growth rates show a negative dependency on K and are sensitive to the level of applied stress.

Acknowledgments: This work was supported by the Director, Office of Basic Energy Sciences, Materials Sciences Division, U.S. Department of Energy under Contract No. DE-ACO3-76SF00098. We thank Dr. D. B. Marshall, D. Malone and T. Yee for helpful discussions and experimental assistance.

REFERENCES

(1) Ritchie, R.O. and Lankford, J., eds., *Small Fatigue Cracks*, TMS-AIME, Warrendale, PA, 1986.

(2) Evans, A.G. in *Fracture Mechanics: New Directions and Perspectives*, ASTM STP 1020, R. P. Wei and R. P. Gangloff, eds., American Society for Testing and Materials, Philadelphia, PA, 1989.

(3) Ritchie, R.O., *Mater. Sci. Eng.*, **103** 15-28 (1988).

(4) Marshall, D.B. and Swain, M.V., *J. Am. Ceram. Soc.*, in press.

(5) Yoda, M., *Int. J. Fract.*, **39** R23-28 (1989).

(6) Jensen, D., Zelizko, V. and Swain, M.V., *J. Mater. Sci. Lett.*, **8** 1154-57 (1989).

(7) Cardona, D.C. and Beevers, C.J., *Scripta Metall.*, **23** 945-50 (1989).

(8) Hoside, T., Ohara, T. and Yamada, T., *Int. J. Fract.*, **37** 47-59 (1988).

(9) Luh, E.H., Dauskardt, R.H. and Ritchie, R.O., *J. Mater. Sci. Lett.*, **8** (1989), in press.

(10) Hannick, R.H.J. and Swain, M.V., *J. Aust. Ceram. Soc.*, **18** 53-62 (1982).

(11) McMeeking, R.M. and Evans, A.G., *J. Am. Ceram. Soc.*, **65** 242-46 (1982).

(12) Budiansky, B., Hutchinson, J.W. and Lambropoulos, J.C., *Int. J. Solids Struct.*, **19** 337-55 (1983).

(13) Newman, J.C., Jr. and Raju, I.S., p. 311 in *Computational Methods in the Mechanics of Fracture*, Chapter 9, vol. 2, S. N. Atluri, ed., Elsevier, 1986.

(14) Dauskardt, R.H., Yu, W. and Ritchie, R.O., *J. Am. Ceram. Soc.*, **70** C248-52 (1987).

(15) Dauskardt, R.H. and Ritchie, R.O., *Closed Loop*, **17** 7-17 (1989).

(16) Dauskardt, R.H., Marshall, D.B. and Ritchie, R.O., *J. Am. Ceram. Soc.*, **72** (1989) in press.

(17) Swain, M.V. and Zelizko, V., in *Advances in Ceramics*, American Ceramic Society, **24**, 1989, in press.

(18) Kawakubo, T. and Komeya, K., *J. Am. Ceram. Soc.*, **70** 400-05 (1987).

(19) Masuda, M., Soma, T., Matsui, M. and Oda, I., *J. Ceram. Soc. Japn. Int. Ed.*, **96** 275-80 (1988).

(20) Swain, M.V., Zelinko, V., Lam, S. and Marach, M., in *Biomaterials*, Prod. MRS Intl. Meeting on Advanced Materials, vol. 1, Materials Research Society, Pittsburgh, PA, 1989, in press.

(21) Dauskardt, R.H., Veirs, D.K. and Ritchie, R.O., *J. Am. Ceram. Soc.*, **72** 1124-30 (1989).

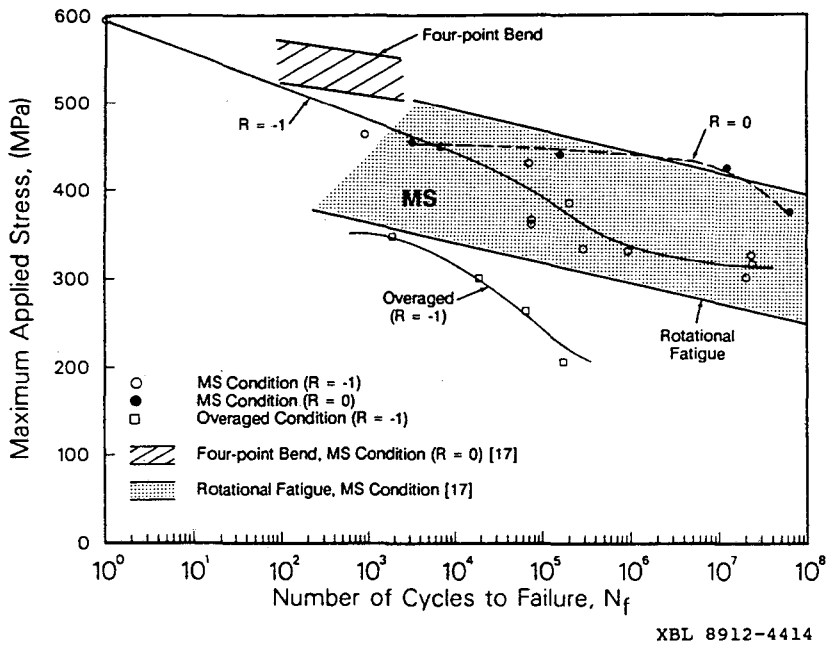

Figure 1. S/N fatigue curves for overaged and transformation-toughened (MS-grade) Mg-PSZ at R = 0 (tension-tension) and -1 (tension-compression). Data from Swain *et al.* (17,20) are shown for comparison.

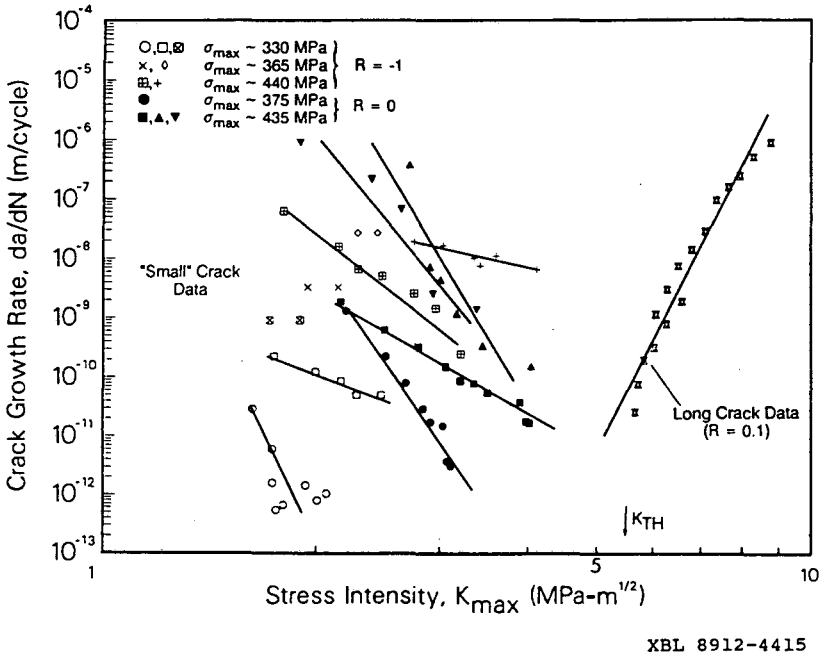

Figure 2. Small-crack growth-rate data in MS-grade Mg-PSZ as a function of K_{max}, showing crack growth well below the long-crack fatigue threshold.

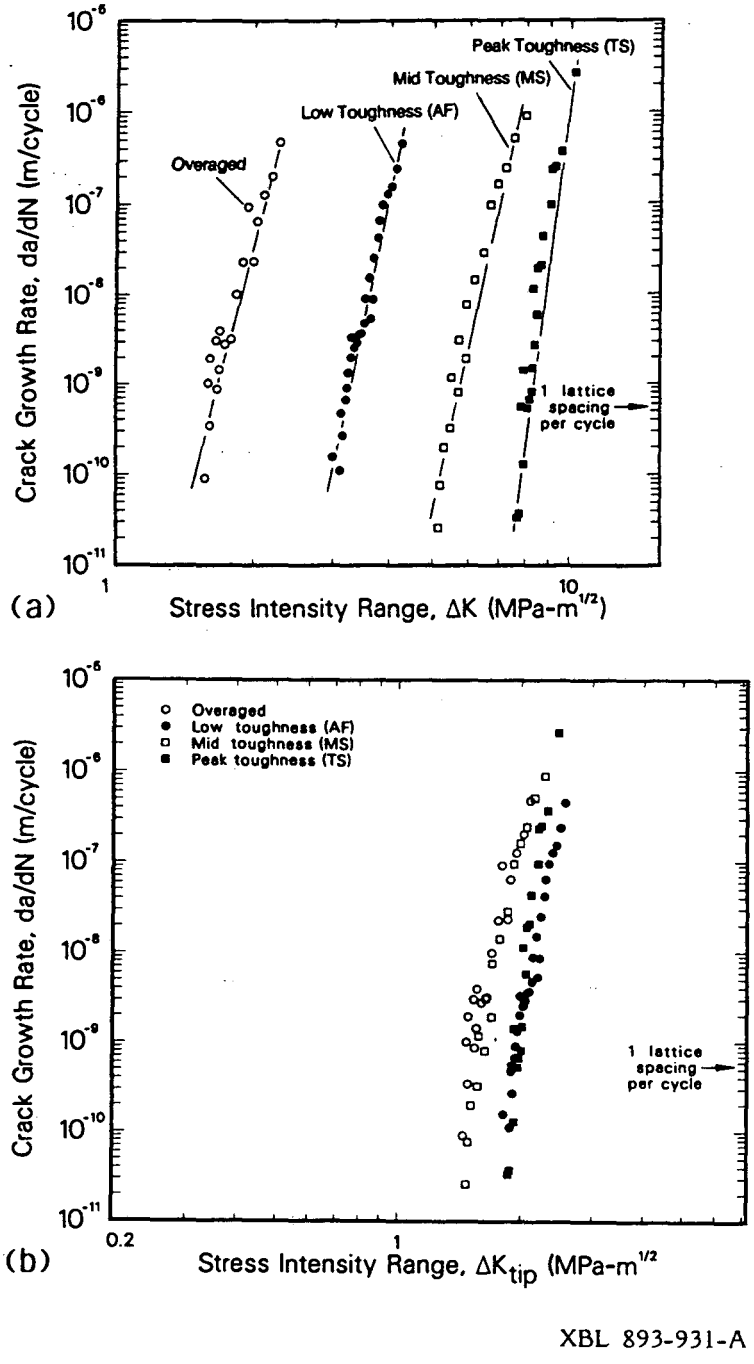

Figure 3. Long-crack growth-rate data in overaged and transformation-toughened Mg-PSZ as a function of a) nominal ΔK and b) near-tip ΔK_{tip} (K_{max}-K_s), showing that cyclic crack-growth resistance is increased with the magnitude of transformation toughening.

LAWRENCE BERKELEY LABORATORY
CENTER FOR ADVANCED MATERIALS
1 CYCLOTRON ROAD
BERKELEY, CALIFORNIA 94720